Edge-coupled InGaAs/InP phototransistors for microwave radio fibre links

J-P. Vilcot, V. Magnin, J. Van de Casteele,
J. Harari, J-P Gouy, B. Bellini, D. Decoster
Institut d'Electronique et de Microélectronique du Nord, UMR CNRS 9929
Avenue Poincaré, BP 69
F-59652 Villeneuve d'Ascq Cedex

Abstract.

Currently, several ways are investigated concerning pico-cellular systems. Although optical feeding of base stations is anyhow involved, there are a lot of microwave signal transmission or generation schemes. Depending on the used scheme, the receiver shall behave differently, either as a pure optoelectronic transceiver (microwave transmission) either as a non-linear optoelectronic system (optical microwave generation, optical locking of microwave oscillator,..). In these fields, we present the work that we did on promising devices, i.e. InP/InGaAs edge-coupled heterojunction phototransistors in two- and three-terminal configuration. Three parts report modelling tools, device technology and characterization. Modelling tools include optical as well as optoelectronic modelling. A brief description of technological work follows. The characterization is made in terms of static response, frequency response and non-linear behaviour.

Modelling tools.

The modelling of heterojunction bipolar phototransistors (HPT's) is made using an optical model in conjunction with an electrical one [1].
The optical model is based on a Finite Difference Beam Propagation Method (FD-BPM) in a two- or three-dimension computational scheme. The electrical one uses a mono-dimensional Energy model in which external circuit as been included.

Optical model.

We use a FD-BPM algorithm in which each layer can have a real or complex refractive index [2]. The reflection coefficient at the air-semiconductor interface has been taken equal to 29%. Light absorption, and so quantum efficiency of the device, is obtained comparing the output light intensity to the input one. Optical injection is made using a 2 μm or 8.5 μm gaussian spotwidth (at 1/e) corresponding to, respectively, a lensed or as-cleaved optical fibre. For laterally symmetric structures (such as PIN photodiodes or 2-T HPT's), two-dimensional FD-BPM is enough to determine the optical behaviour of the structure. For asymmetric ones (such as 3-T HPT's), three-dimensional algorithm is sometimes preferred in order to obtain a more realistic optical field profile. As examples, we present:
- in **Fig.1**, the light propagation inside a 2-T HPT (2D FD-BPM), the use of a lensed fibre increases the quantum efficiency from 13% to 43% (@ 1.55 μm) compared to a cleaved one,
- in **Fig.2**, the light propagation inside a 3-T HPT (3D FD-BPM), the use of an InGaAsP subcollector instead of an InP one increases the quantum efficiency from 37.5% to 61% (lensed fibre @ 1.3 μm)(40% to 63% @ 1.55 μm in the same conditions).
From these propagation results, the carrier generation rate due to optical absorption can be deduced at any distance along the propagation axis. **Fig. 3** shows the carrier generation rate which is obtained for the 3-T HPT when illuminated with a lensed and as-cleaved fibre. The

sensitivity to optical injection, i.e. the effect of fibre misalignment, can also be computed. **Fig. 4** shows the device efficiency modification versus lensed fibre deviation; a more sensitive position effect (1μm deviation cuts the efficiency by a factor 2) is obviously observed compared to an as-cleaved fibre.

Electrical model.

A mono-dimensional Energy model based on Boltzmann transport equation [2, 3] is used to determine the physical behaviour of the devices. They are shared into elementary slices along propagation axis; the optical generation rate, obtained from the optical model (see Fig. 3), is inserted into each slice. We must point out that, using such a mono-dimensional model, we can not consider transport phenomena which could occur due to the variation of generation rate along the propagation axis; so, we assumed that there is no carrier displacement along this axis. Each elementary currents are added to obtain the total current of the device. Another thing to point out is the fact that a simplified generation rate (constant generation over the 4-5 first microns and no generation after) gives no significant difference in the results: the great advantage is a smaller computational time. The whole electrical behaviour is obtained by including the external circuit effect. Base potential can be floating (2-T HPT's) either voltage or current driven (3-T HPT's). The model can be used either for the design of the device (particularly epitaxy) or the device performance (static and dynamic).

Device technology.

The two types of transistors were fabricated on the following epitaxy:

emitter	n-InGaAs, 50 nm, $5x10^{18}$ cm^{-3}
	n-InP, 1.35 μm, $5x10^{18}$ cm^{-3} (only 3-T HPT)
	n-InP, 0.15 μm, $5x10^{17}$ cm^{-3}
spacer	n-InGaAs, 20 nm, $5x10^{15}$ cm^{-3}
base	p-InGaAs, 0.1 μm, 10^{19} cm^{-3}
collector	n-InGaAs, 0.4 μm, $5x10^{15}$ cm^{-3}
sub-collector	n-InP, 0.5 μm, $2x10^{18}$ cm^{-3}
substrate	n-InP

2-T HPT.

First, ridges of 6 μm are dry etched down to InP subcollector layer. Polyimide (2μm) and resist (3 μm) films are then deposited in order to planarize the structure. Etching of these layers are stopped right to the top of the ridges, no mask is required but accurate control is needed. A second photolithographic step defined the emitter contact. A dry etch self-aligned on the top electrode was then performed in order to isolate HPT's from each other. As last steps, thinning of substrate and backside collector contact were made.

3-T HPT.

Emitter ohmic contact (2μm, 4μm, and 6 μm wide) is first deposited and acts as mask for emitter etch. A mixing of dry and wet etches is used in order to obtain a very small underetching. This one allowed a self-aligned base metallisation step, the gap between base metal and emitter is close to 0.2 μm. Base mesa is then made followed by a planarization step identical to the one use for the 2-T HPT. Subsequent etches are made in order to contact emitter and base. Thinning and collector backside electrode concluded the process. The length of devices is fixed by cleaving and is between 4 and 15 μm. **Fig. 5** represents a SEM view of a 4 μm x 8 μm device.

Device characterization.

Static characterization.

The static characteristics of HPT's are shown on **Fig. 6a & 6b** for, respectively, 2-T and 3-T devices. For 2-T HPT's, external responsivity is around 4 to 5 A/W (as-cleaved fibre @ 1.3 μm) for bias voltage of 1V (using a lensed fibre, external responsivity reaches 12 A/W). Since the external quantum efficiency has been evaluated around 0.1 by comparison with a PIN photodiode of equivalent structure, we can deduce an internal gain value about 40 (@ 1V). We can notice that, due to different optical confinement conditions inside the device, the external responsivity is around 4 A/W at 1.55 μm. For 3-T HPT, the external responsivity of the base-collector junction used as PIN photodiode has been measured equal to 0.14 A/W (@ 1.3 μm) which corresponds to theoretical predictions. Referring to this measurement, and to the responsivity of the transistor, under current controlled base electrode operation, which value is around 8 A/W (@ 500μA base current), a maximum intrinsic DC gain value around 55 is obtained (**Fig.7**). The use of a lensed fibre allows responsivity to reach 24 A/W but the misalignment is much more sensitive that for as-cleaved fibre.

Dynamic characterization.

Frequency response.

Frequency response of devices has been measured up to 15 GHz. Reference is taken using a 1014A New Focus photodiode exhibiting a responsivity of 0.25 A/W and a cut-off frequency of 40 GHz. **Fig. 8a & 8b** shows the response of the 2-T and 3-T HPT's. Their respective optical unity gain frequency has been evaluated to 25 GHz and 40 GHz. As already reported [4], 2-T HPT's show a continuously decreasing frequency response. In the case of 3-T HPT, the response is strongly dependent on the base external circuit (resonant circuits can be used in order to obtain tuned photoreceivers [5]). For the experiment reported in **Fig. 8b**, the external circuit is a 50 Ω resistor: this explains the lower gain obtained compared to 2-T HPT but also the relatively flat response.

Non-linear behaviour.

The non-linear behaviour of 2-T HPT's has already been reported [6, 7]. Here we give two examples of experiments carried out using two optical beams. In a first one, one was RF modulated and the other one CW. Depending on CW beam power, the RF output level of the device can be modified. As an example, for 1 mW CW power impinging on the device, an increase of 18 dB at 500 MHz and 14 dB at 5 GHz has been measured by comparison to no illumination conditions. In a second experiment, two modulated light beams were focused on the device, one is 2 GHz RF modulated and the other is 2 KHz square modulated. The resulting output power is given on **Fig. 9** where we can observe the total modulation of the 2 GHz signal by the 2 KHz square one.

For 3-T HPT's, depending on impinging light power and base current, very non-linear behaviour has been observed specially for low light powers. As example, when compared to the case where no base current is injected, the output level (corresponding to a 1 GHz modulated light beam) shows up to 30 dB improvement at impinging light powers around 10 μW and base current of 0.5 mA. Mixing experiments of RF optically and electrically generated signals have been carried out. A 1 GHz optically generated sub-carrier has been mixed with a 18 GHz electrical carrier (-20 dBm), the output signal of HPT is given on **Fig. 10**. An other experiment was performed using a 8 GHz modulated optical signal mixed with an electrical signal which frequency is in between 500 MHz and 10 GHz (-10 dBm). An up-conversion gain around 6 dB has been obtained at 500 MHz and 0 dB gain is around 6 GHz.

Electrical equivalent circuit.

The S parameters have been measured up to 15 GHz due to the limitations of the microwave submount used. From these measurements a small signal equivalent circuit has been deduced. The optical input is introduced as a current generator between emitter and collector. Due to electrode configuration, important parasitic capacitances exist between base and collector and between emitter and collector. This shall be overcome by the use of a semi-insulating substrate. A large signal equivalent circuit has also been made: each equivalent circuit element value depending on base current which is a combination of electrical and photogenerated ones.

Conclusion.

From this study, edge-coupled HPT's appear to manage microwave functionality in both linear and non-linear applications as well as high responsivity. Nevertheless, some improvements can be:

- the use of an InGaAsP subcollector; this tend to a better optical efficiency,
- the use of a semi-insulating substrate; this shall give low parasitic capacitance devices. However, technology would be more difficult especially concerning the electrode design since the edge-coupling technique implies some restrictions concerning the electrical connections. Such devices are currently under design.

We have to keep in mind that such edge-coupled devices need always some kind of drastic alignment scheme. The use of an optical waveguide illumination, such as an evanescently coupled optical waveguide [8], can bring two major advantages: no precise cleaving of devices is needed and the compatibility with HBT MMIC technology can be increased [9].

References:

[1] V. Magnin, J. Van de Casteele, J. Harari, J-P. Gouy, S. Maricot, J-P. Vilcot, D. Decoster, "Study of edge-coupled waveguide InGaAs/InP heterojunction phototransistors for microwave applications", *Proc. of Fibre Optics in Microwave Systems and Radio Access IEE Conf.*, 1997, pp. 4/1-4/6

[2] J. Harari, F. Journet, O. Rabii, G. Jin, J-P. Vilcot, D. Decoster, "Modeling of waveguide PIN photodetectors under very high optical poweer", *IEEE Trans. on Microwave Theory and Techniques*, 1995, Vol. 43(9), pp. 2304-2310

[3] C. Dalle, P-A. Rolland, "Drift-diffusion versus Energy model for millimetre-wave IMPATT diodes modelling", *Intern. Journ. Of Numerical Modelling: Electronic networks, Devices and fields*, 1989, Vol. 2, pp. 61-73

[4] D. Wake, D.J. Newson, M.J. Harlow, I.D. Henning, "Optically-biased, edge-coupled InP/InGaAs heterojunction phototransistors", 1993, *Electronics Letters*, Vol. 29(25), pp. 2217-2219

[5] H. Kamitsuma, "Ultra-wideband monolithic photoreceivers using HBT-compatible HPT's with novel base circuits, and simultaneously integrated with an HBT amplifier", *IEEE Journal of Lightwave Technology*, 1995, Vol. 3(12), pp. 2301-2307

[6] J. Van de Casteele, J.P. Vilcot, J.P. Gouy, F. Mollot, D. Decoster, "Electro-optical mixing in an edge-coupled GaInAs/InP heterojunction phototransistor", *Electronics Letters*, 1996, Vol. 32 (11), pp. 1030-1032

[7] C.P. Liu, A.J. Seeds, D. Wake, "Two-terminal edge-coupled InP/InGaAs heterojunction phototransistor optoelectronic mixer", *IEEE Microwave and guided wave Letters*, 1997, Vol. 7 (3), pp. 72-74

[8] D.P. Prakash, D.C. Scott, R. Fetterman, M. Matloubian, Q. Du, W. Wang, "Integration of polyimide waveguides with travelling-wave phototransistors", *IEEE Photonics Techn. Lett.*, 1997, Vol. 9 (6), pp. 800-802

[9] D. Streit, L. Tran, R. Lai, Y. Chen, J. Cowles, K. Kobayashi, A. Oki, T. Block, M. Barksy, P.H. Liu, J. Elliot, " An InP-based HEMT and HBT MMIC production line", *Proc. of 5th European. Gallium Arsenide and Rel. Comp. Appl. Symp., GAAS 97*, 1997, pp. 59-63.

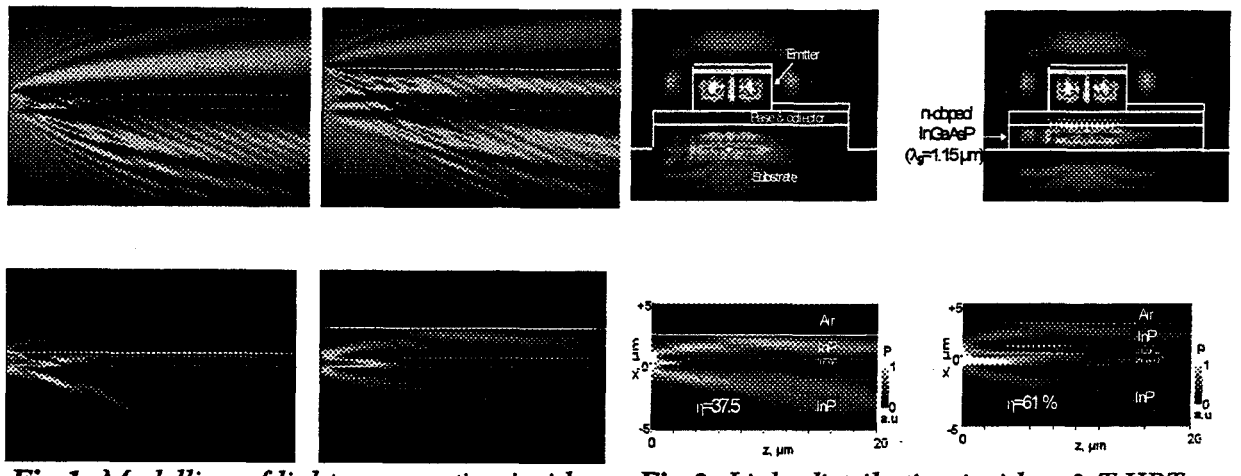

***Fig.1**: Modelling of light propagation inside a 2-T HPT structure @ 1.3 μm LEFT: thin emitter. RIGHT: thick emitter. TOP: as-cleaved fibre. BOTTOM lensed fibre.*

***Fig.2**: Light distribution inside a 3-T HPT structure (lensed fibre @ 1.3 μm) LEFT: InGaAs collector. RIGHT: InGaAs & InGaAsP collector. TOP: cross-sectional profile. BOTTOM: along propagation axis*

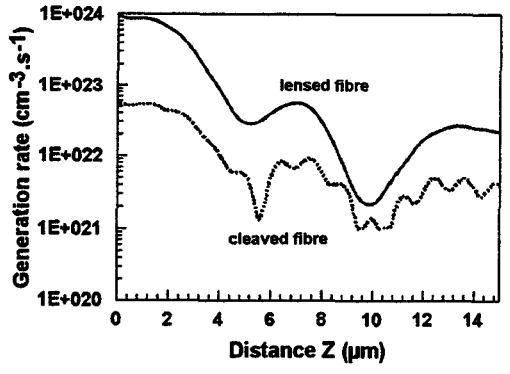

***Fig. 3**: Optical generation rate along the propagation axis. Optical input power is 1 μW, air-semiconductor reflection coefficient is 29%.*

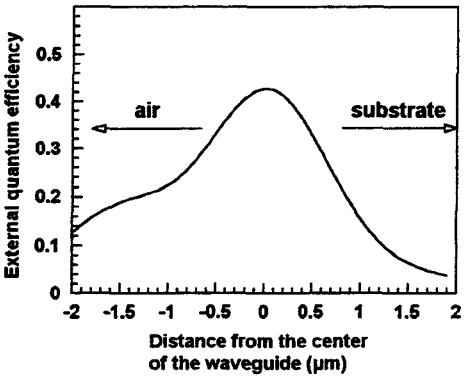

***Fig. 4**: External quantum efficiency of 3-T HPT (lensed fibre illumination @ 1.3 μm) versus fibre misalignment relative to optical waveguide centre.*

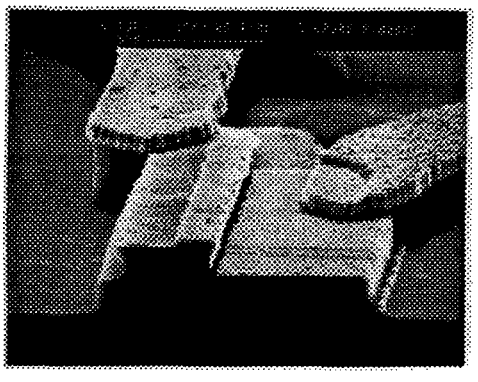

***Fig. 5**: SEM view of 4 μm x 8 μm edge-coupled 3-T HPT (collector is backside).*

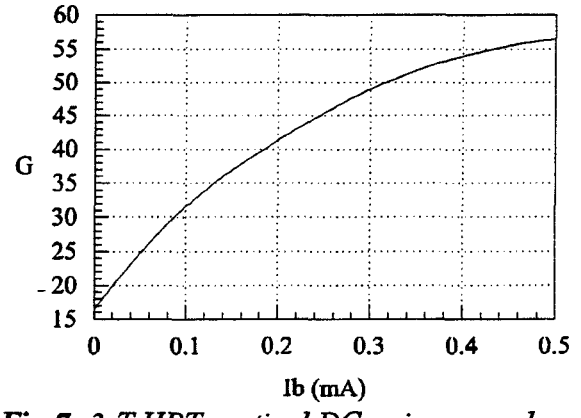

***Fig.7**: 3-T HPT: optical DC gain versus base current (1mW optical power @ 1.3 μm)*

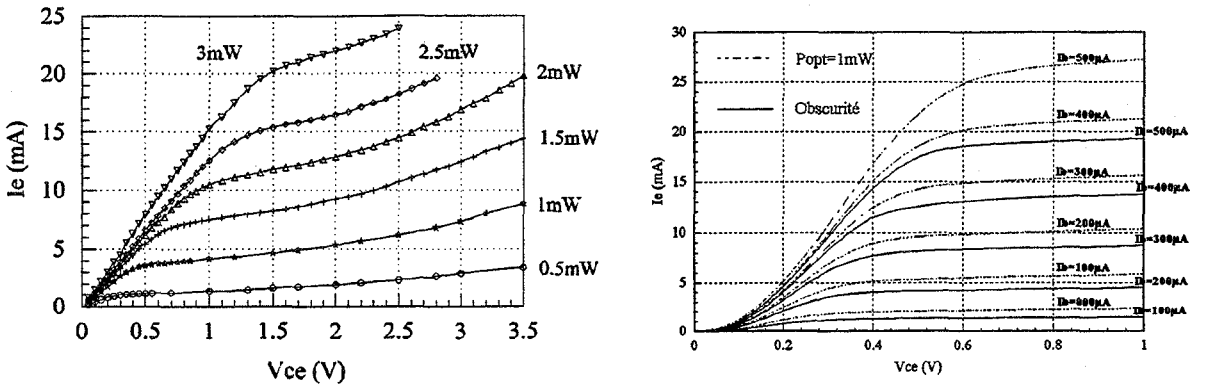

a) *b)*

Fig. 6: *Static characteristics of 2-T and 3-T HPT's (as-cleaved fibre @ 1.3μm).*

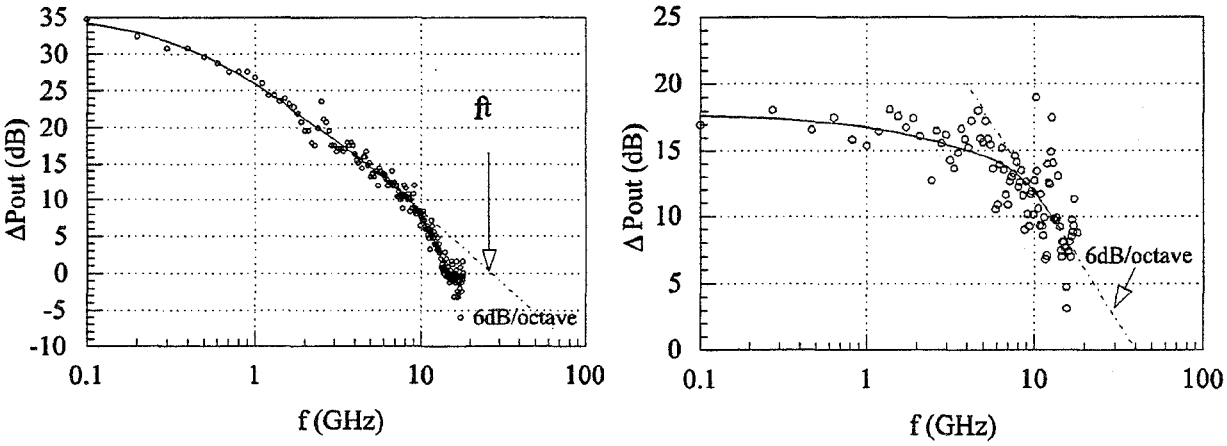

a) *b)*

Fig8: *Frequency response of 2-T (a) and 3-T (b) HPT's. 0 dB corresponds to the output power of a 1014A New Focus photodetector.*

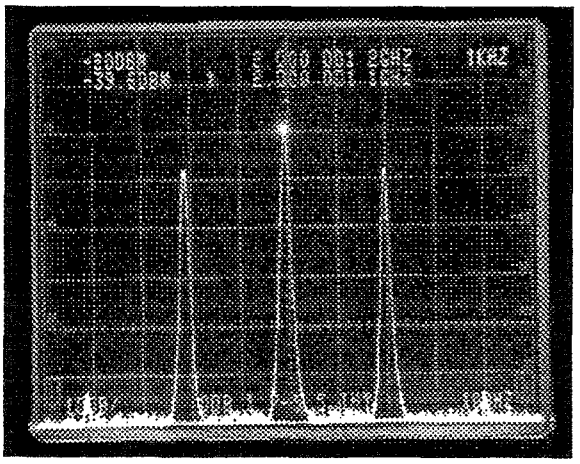

Fig. 9: *Output signal of a 2-T HPT illuminated by a 2 GHz modulated light beam and a 2 KHz one.*

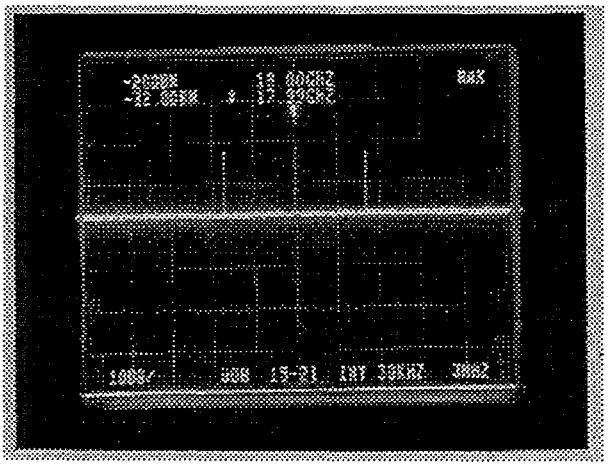

Fig. 10: *Output signal of a 3-T HPT illuminated by a 1 GHz modulated light beam and biased with a 18 GHz electrical signal*